MAGNETIC RESONANCE IN CHEMISTRY, VOL. 36, 13–34 (1998)

Investigation of the Decomposition of Compounds Containing Azo Groups by EPR Spectroscopy

A. Staško,[1]* K. Erentová,[1] P. Rapta,[1] O. Nuyken[2] and B. Voit[2]

[1] Department of Physical Chemistry, Slovak Technical University, Radlinského 9, SK-812 37 Bratislava, Slovak Republic
[2] Lehrstuhl für Makromolekulare Stoffe, Technische Universität München, Lichtenbergstr. 4, D-85747 Garching, Germany

Received 24 March 1997; revised 10 July 1997; accepted 28 July 1997

ABSTRACT: In photochemically, electrochemically and thermally initiated decomposition, compounds containing the azo group ($^1RN{=}N^2R$) usually form reactive, short-lived radicals $^1R^{\cdot}$ and $^2R^{\cdot}$, which corresponds to synchronous splitting. As examples, aliphatic azo compounds, 1-aryl-2-alkylazo compounds, azophosphonates, azosulfonates, azosulfones, azosulfides, triazenes, pentazadienes, hexazadienes, acyl- and diacylazo compounds, diazonium salts and cyclic azo compounds have been studied. $^1R^{\cdot}$ and $^2R^{\cdot}$ were characterized by means of the EPR spin trap technique. These reactive radicals may abstract hydrogen from the solvent or any neighborhood functions, or dimerize ($^1R{-}{-}^2R$). Some azo compounds trap $^1R^{\cdot}$ and $^2R^{\cdot}$ and thus form the corresponding hydrazyl radicals. In cathodic reduction, prior to the initiation of decomposition, corresponding anion radicals centered on the azo group were observed which have considerable stability if ^1R and ^2R are conjugated structures. © 1998 John Wiley & Sons, Ltd.

KEYWORDS: EPR; ESR; azo compounds; free radicals; spin trap

INTRODUCTION

Considerable interest in azo compounds ($^1RN{=}N^2R$) has been stimulated by their potential applications in polymer chemistry and as optical data storage materials.[1] Azo compounds are well known as a source of alkyl and aryl radicals in thermally, photochemically and electrochemically initiated decomposition. Only a few papers have reported on the investigation of the decomposition of azo compounds using the EPR spin trap technique. Thus, originally, the thermal, photochemical and chemical decomposition of a variety of azoalkanes such as phenylazotriphenylmethane (PAT)[2–11] were investigated using nitrone (5,5-dimethylpyrrolidine-1-oxide, α-phenyl-*N*-*tert*-butyl nitrone) and nitroso (2-methylnitrosopropane, nitrosodurene) spin traps. Kobayashi *et al.*[12] described free radicals photochemically generated from arylazo *p*-tolyl sulfones by means of the 2-methylnitrosopropane spin trap. Numerous variously substituted phenyl radicals were trapped by the decomposition of arenediazonium salts.[13–16] Generally, two radical mechanisms for azo group splitting are assumed: synchronous ($^1R{-}{-}N_2{-}{-}^2R \rightarrow {}^1R^{\cdot} + N_2 + {}^2R^{\cdot}$)[17] and asynchronous ($^1R{-}{-}N_2{-}{-}^2R \rightarrow {}^1RN_2^{\cdot} + {}^2R^{\cdot}$).[18] The formation of $RN_2^{\cdot}$ radicals was unambiguously confirmed by Suehiro *et al.*[19] in the photochemically initiated decomposition of azo sulfides and triazenes in cyclopropane at low temperatures using EPR spectroscopy. In the cathodic reduction and anodic oxidation of azo compounds, the formation of the corresponding anion and cation radicals were observed.[20] Some are stable, but most of them decompose to form reactive radicals $^1R^{\cdot}$ and $^2R^{\cdot}$.

The aim of this paper is to summarize our EPR results obtained in the photochemically,[21–28] electrochemically[29–32] and thermally initiated[32,33] decomposition of novel azo group-containing compounds recently synthesized in these laboratories. The reactive radical splitting products and their consecutive reactions were studied using the spin trap technique.[34–36]

EXPERIMENTAL

The compounds we investigated are shown in Fig. 1. Sources and methods of preparation are described in more detail in appropriate references. They are aliphatic azo compounds (**I**), azosulfonates (**IV**), azosulfones (**V**) and diazonium salts (**XI**),[22] azosulfides (**VI**),[25] 1-aryl-2-alkylazo compounds (**II**), azophosphonates (**III**), triazenes (**VII**), acyl- and diacylazo compounds (**X**) and cyclic azo compounds (**XII**),[32] pentazadienes (**VIII**)[37] and hexazadienes (**IX**).[38]

The solvents employed, acetonitrile (CH_3CN), methanol (MeOH), ethanol (EtOH), benzene, toluene, dichloromethane (CH_2Cl_2) and dimethyl sulfoxide

* Correspondence to: A. Staško, Department of Physical Chemistry, Slovak Technical University, Radlinského 9, SK-812 37 Bratislava, Slovak Republic.
Contract/grant sponsor: Slovak Grant Agency; *Contract grant number*: VEGA 1/4206/97.

 CCC 0749-1581/98/010013–22 $17.50

I. Aliphatic azocompounds

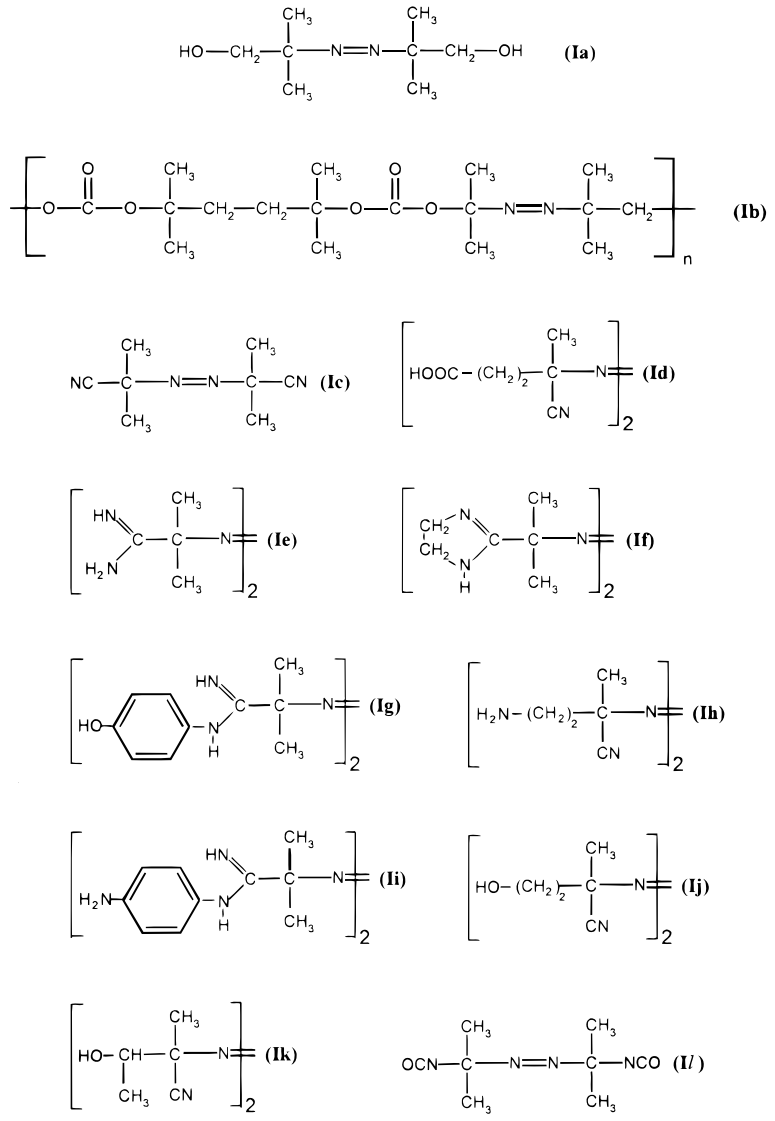

Figure 1. Azo group-containing compounds I–XII.

(DMSO), were commercial products of analytical purity purchased from Aldrich. The spin traps, 2-methyl-3-nitrosopropane (^{t}BuNO), nitrosodurene (ND) and 5,5-dimethylpyrroline-*N*-oxide (DMPO) were purchased from Sigma.

In the photochemical and thermolysis experiments, solutions containing 10^{-3} M or saturated substrate solutions were used under argon. Most of the experiments were carried out *in situ*, directly in the cavity of an EPR spectrometer at 295 K using a medium-pressure mercury lamp (from Applied Photolysis, UK) as an irradiation source, or a Bruker variable-temperature unit for thermal decomposition.

Electrochemical reduction was performed mostly in CH_3CN solutions containing 0.001 M substrate and 0.1 M tetrabutylammonium perchlorate (TBAP) under argon, directly in the cavity of an EPR spectrometer on a platinum net, using a Varian electrolytic cell.

EPR spectra were recorded and also simulated by employing a Bruker 200D spectrometer on-line with an Aspect 2000 computer.

RESULTS AND DISCUSSION

Photolysis

Generally, in the photochemically initiated decomposition of the investigated series of azo group-containing compounds **I**, **II** and **IV**–**XI**, radical products corresponding to synchronous decomposition ($^1R—N_2—^2R \rightarrow {}^1R^{\cdot} + N_2 + {}^2R^{\cdot}$) were observed (Table 1). The radical intermediates $RN_2^{\cdot}$ expected from asynchronous splitting were not found, probably owing to their very limited stability. Radicals $^1R^{\cdot}$ and $^2R^{\cdot}$ are of very short lifetime; however, it was possible to identify them by means of the spin trap agents (^{t}BuNO, ND and DMPO) as described below.

II. 1-Aryl-2-Alkyl azocompounds

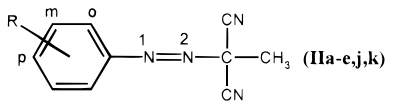

(IIa-e,j,k)

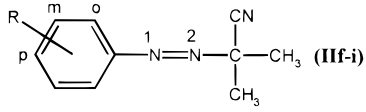

(IIf-i)

Probe	IIa	IIb	IIc	IId[a]	IIe[a]
R	H	*p*-NO_2	*p*-CH_3O	*o*-NO_2	*m*-COOH
Probe	IIf	IIg	IIh	IIi	IIj
R	*p*-NO_2	*o,o*-Cl_2	*p*-Br	*p*-H	*p*-CH_2OH

a) ^{15}N labelled compound

R = 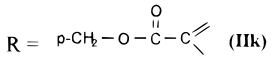

(IIk)

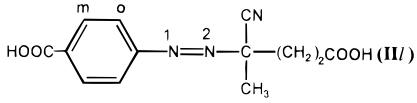

(II*l*)

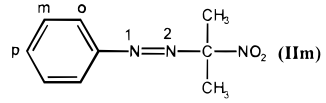

(IIm)

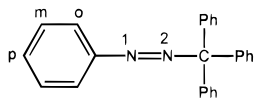

(IIn)

III. Azophosphonates

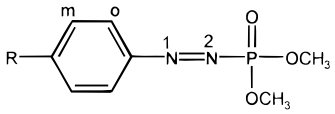

(IIIa-f)

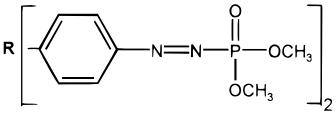

(IIIg-i)

Probe	IIIa	IIIb[a]	IIIc	IIId	IIIe	IIIf
R	H	H	Cl	CH_3O	CH_3	CH_3OC
Probe	IIIg	IIIh	IIIi			
R	-	-O-	-CO-			

a) ^{15}N labelled compound

Figure 1. Continued

^{t}BuNO. Identification of radicals $^1R^\cdot$ and $^2R^\cdot$ was carried out using spin traps such as ^{t}BuNO as illustrated in Fig. 2. The left half represents the experimental trace and the right half the simulated EPR spectrum of the radical adducts to ^{t}BuNO [except for Fig. 2(b); see later]. The *g*-values (around 2.0057) and relatively high nitrogen hyperfine splitting constants ($a_N > 1$ mT) are characteristic parameters for the nitroxyl group. Spectra have characteristic triplet pattern (1:1:1). Hyperfine splitting structures indicate the presence of the phenyl ring with the highest splitting constant for the *para* and *ortho* protons ($a_H^{p,\,o,\,o} \approx 0.17$ mT) and considerably lower splittings for the *meta* protons ($a_H^{m,\,m} \approx 0.08$ mT) as shown in Fig. 2(a). Upon replacement of *meta* [Fig. 2(c)] or *para* [Fig. 2(d)] protons with the —OCH_3 group, the corresponding contribution of protons to the hyperfine structure is eliminated. The hyperfine structure in Fig. 2(e), in addition to splitting from the *ortho* and *meta* protons, shows the contribution of the nitrogen atom from the nitro group in the *para* position with $a_N =$ 0.053 mT. The hyperfine structure in the spectrum in Fig. 2(f) is missing. We assume that the spectrum originates from the ^{t}BuNO$^\cdot$–SO_3Na adduct, as under analogous experimental conditions we unambiguously identified the $^\cdot SO_3$Na radical by means of the DMPO spin trap. However, here the formation of $^tBu_2NO^\cdot$, having similar parameters, cannot be excluded.

A deviation from the standard behavior was observed in the decomposition of **IVc**, probably due to steric hindrance by the *ortho*-substituted phenyl group. The coplanarity with the NO group is removed and consequently only very small splittings are observed in the experimental spectrum [Fig. 2(b)]. In addition, further unidentified superimposed spectra are evident in Fig. 2(b) and (d) marked with ×, $2 \times a_H = 0.498$ mT. This value is consistent with the $^\cdot CH_2OX$ adduct to ^{t}BuNO, where X is phenyl from the azo compound. The participation of the solvent in this case is improbable since the experiment with CD_3OD and CH_3OH did not produce any changes in the splitting constants of the radical.

DMPO. The type of radical trapped with DMPO depends decisively on whether the decomposition is carried out in air or in an argon atmosphere.[10] Whereas

IV. Azosulfonates

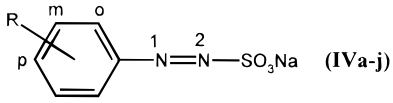

(IVa-j)

Probe	IVa	IVb[a]	IVc	IVd	IVe
R	H	H	*o*-CH_3O	*m*-CH_3O	*p*-CH_3O
Probe	IVf	IVg	IVh	IVi	IVj
R	*m,m*-$(COOCH_3)_2$	*m,m*-$(COOH)_2$	*m*-CH_3	*p*-OH	*p*-NH_2

a) ^{15}N labelled compound

V. Azosulfones

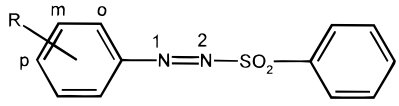

(Va-e)

Probe	Va	Vb	Vc	Vd	Ve
R	H	*m*-CH_3	*p*-CH_3	*p*-Cl	*p*-NO_2

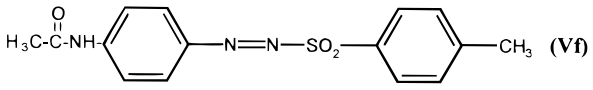

(Vf)

VI. Azosulfides

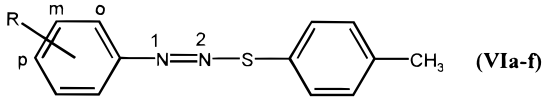

(VIa-f)

Probe	VIa	VIb	VIc	VId	VIe	VIf
R	*p*-NO_2	*m*-NO_2	*o*-NO_2	*m*-COOH	*m,m*-$(COOH)_2$	*p*-SO_3H

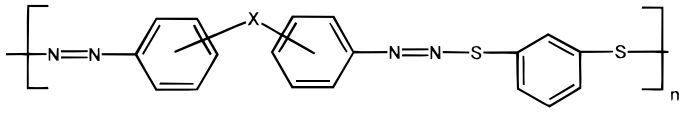

(VIg-j)

Probe	VIg	VIh	VIi	VIj
X	*p*(-O-)	*p*(-CO-)	*p*(-SO_2-)	*m*(-SO_2-)

Figure 1. Continued

the azosulfonates generally give the corresponding substituted phenyl and $^{\cdot}SO_3Na$ radical adducts in air and argon, the aliphatic azo compounds with tertiary carbons such as **I** are very sensitive to the presence of oxygen, as illustrated in Fig. 3. Water-soluble compounds such as **Ie**, **f**, **g** and **i** irradiated in air form hydroxyl radicals during the initial stages of irradiation, as illustrated with the characteristic $^{\cdot}$DMPO–OH adduct in Fig. 3(a). Upon prolonged irradiation (after oxygen consumption), the relative concentration of carbon-centered adducts $^{\cdot}$DMPO–$CR^1R^2R^3$, which are exclusively formed under an argon atmosphere, increases. If the compounds with a tertiary carbon are photolysed in benzene in the presence of oxygen, no carbon-centered adducts but $^{\cdot}$DMPO–O_2–$CR^1R^2R^3$ adducts are formed in high concentrations with characteristic spectra as shown in Fig. 3(c).

Nitrosodurene. In addition to ^{t}BuNO and DMPO, nitrosodurene was also used in the investigation of the photolysis of azo group-containing compounds. This is illustrated in Fig. 4 with the photolysis of thioazo compounds **VI**. Using substrates **VIa–c**, the $^{\cdot}SC_6H_4CH_3$ radical is evident, together with the solvent radical $^{\cdot}CH_2CN$ [Fig. 4(a)], which was formed by abstracting a proton from acetonitrile. If azo compound **VIf** was

VII. Triazenes

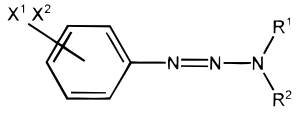

(VIIa-i)

Probe	X^1	X^2	R^1	R^2
VIIa	*m*-COOH	H	C_2H_5	C_2H_5
VIIb	*m*-COOH	H	CH_3	CH_2CH_2OH
VIIc	*m*-COOH	H	$CH(CH_3)_2$	$CH(CH_3)_2$
VIId	*m*-COOH	H	$CH_2CH_2CH_3$	$CH_2CH_2CH_3$
VIIe	*m*-COOH	*m'*-COOH	C_3H_5	C_2H_5
VIIf	*m*-COOH	*m'*-COOH	CH_2CH_2OH	CH_2CH_2OH
VIIg	*m*-CON_3	*m'*-CON_3	C_2H_5	C_2H_5
VIIh	*p*-COOH	H	C_2H_5	C_2H_5
VIIi	*p*-CN	H	C_2H_5	C_2H_5
VIIj	*p*-NO_2	H	C_2H_5	C_2H_5

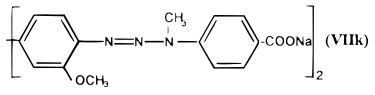

(VIIk)

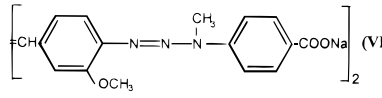

(VIIl)

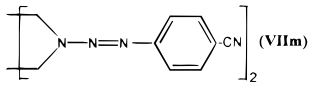

(VIIm)

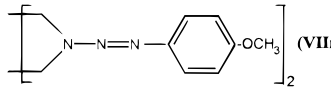

(VIIn)

VIII. Pentazadienes

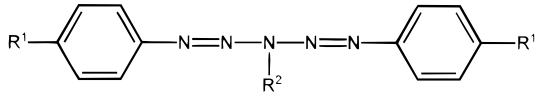

(VIIIa-e)

Probe	VIIIa	VIIIb	VIIIc	VIIId	VIIIe
R^1	H	CH_3	OCH_3	Cl	NO_2
R^2	C_2H_5	C_2H_5	C_2H_5	C_2H_5	n-Bu

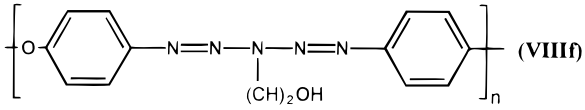

(VIIIf)

Figure 1. Continued

used, then in addition to $^{\cdot}ND–SC_6H_4CH_3$ and $–CH_2CN$, also the $^{\cdot}ND–C_6H_4\,pSO_3H$ radical was found [Fig. 4(b)], with the characteristic hyperfine structure of phenyl protons superimposed on the spectra as already shown in Fig. 4(a). The disadvantage of ND of its relatively low solubility was compensated for in the investigated system by the high photochemical stability of ND itself and its adducts.

Azo compounds as spin traps. Azo compounds **IV**, soluble in polar solvents (water, ethanol), photolytically decompose to aryl ($^1R^{\cdot}$) and $^{\cdot}SO_3Na$ ($^2R^{\cdot}$) radicals, but simultaneously these compounds also trap radicals to form the spin adducts $^1R—N(X)—N^{\cdot}—SO_3Na$ (Table 2), where X is $NaSO_3$ in water at 275 K and H in EtOH at 320 K. The half-lives of these radicals are between 0.1 and 2 s. Figure 5(a) and (b) illustrate the experimental and simulated EPR spectra found in the decomposition of **IVa** and its ^{15}N analogue **IVb** in water solution at 275 K. The assignment of splitting constants to phenyl as stated in Table 2 is based on the systematic substitution of the phenyl ring with an OCH_3 group, where the corresponding proton splittings were eliminated. The assignment of nitrogen splittings was confirmed from ^{15}N substitution. There is non-homogeneous line broadening towards the outer lines, pointing to hindered rotation around the —N—N— group. This was studied in the simulation by using different peak-to-

IX. Hexazadienes

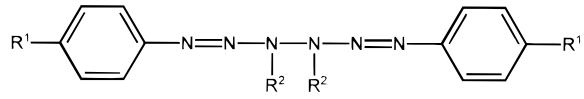

(IXa-d)

Probe	IXa	IXb	IXc	IXd
R^1	Cl	Cl	$COCH_3$	$COOC_2H_5$
R^2	$COCH_3$	CH_3	CH_3	CH_3

X. Acyl- and Diacylazocompounds

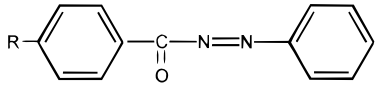

(Xa-c)

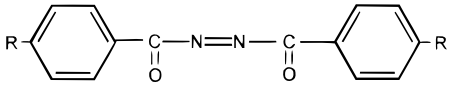

(Xd-f)

Probe	Xa	Xb	Xc	Xd	Xe	Xf
R	H	Cl	CH_3	H	Cl	CH_3

XI. Diazonium salts

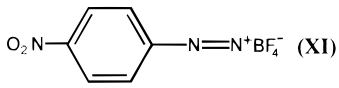

(XI)

XII. Cyclic azocompounds

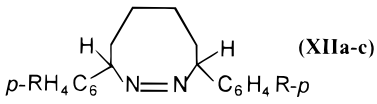

(XIIa-c)

Probe	XIIa	XIIb	XIIc
R	H	CH_3	CH_3O

Figure 1. Continued

peak widths (*pp*) and amplitudes (Y_m) for outer (*pp* = 0.024 mT, $Y_m = 0.4$) and middle lines (*pp* = 0.015 mT, $Y_m = 1$).

Figure 5(c) shows experimental and simulated EPR spectra observed in the photolysis of **IVa** in EtOH at 320 K. From the analysis of the splitting constants summarized in Table 2 it is evident that the corresponding radical Ph—N(H)—N˙—SO_3Na represents the hydrogen spin adduct to the original azo compound. To elucidate the origin of the hydrogen we carried out the experiments with variously deuterated ethanols. The spectrum observed in EtOD [Fig. 5(d)] confirms the origin of hydrogen is the ethanol molecule. This H abstraction probably proceeds via the photochemically activated complex of the azo compound with ethanol.

Miscellaneous. Most of the reactions and radical products described above are characteristic of a certain group of azo compounds. However, numerous additional radicals were also found, which cannot be incorporated in a general decomposition scheme, or for which the identification is ambiguous. Only a few of them are listed in Table 1.

Electrolysis

In the electrolytic reduction or oxidation of azo compounds, the corresponding anion radicals and cation radicals are formed. Some anion radicals are stable but most of them decompose to reactive radicals $^1R^\cdot$ and $^2R^\cdot$ with the elimination of nitrogen ($^1RN_2{}^2R^{-\cdot} \rightarrow {}^1R^\cdot + N_2 + {}^2R^-$ or $^1R^- + N_2 + {}^2R^\cdot$). Generally, the cation radicals of azo compounds are very unstable and were not observed in our studies. Azoalkane radical cations, except for such special structures as azonorbornane, are short lived and their EPR spectra have been mostly observed under matrix isolation conditions at low temperatures.[39–48] Similarly to the photochemically initiated decomposition, radicals $^1R^\cdot$ and $^2R^\cdot$

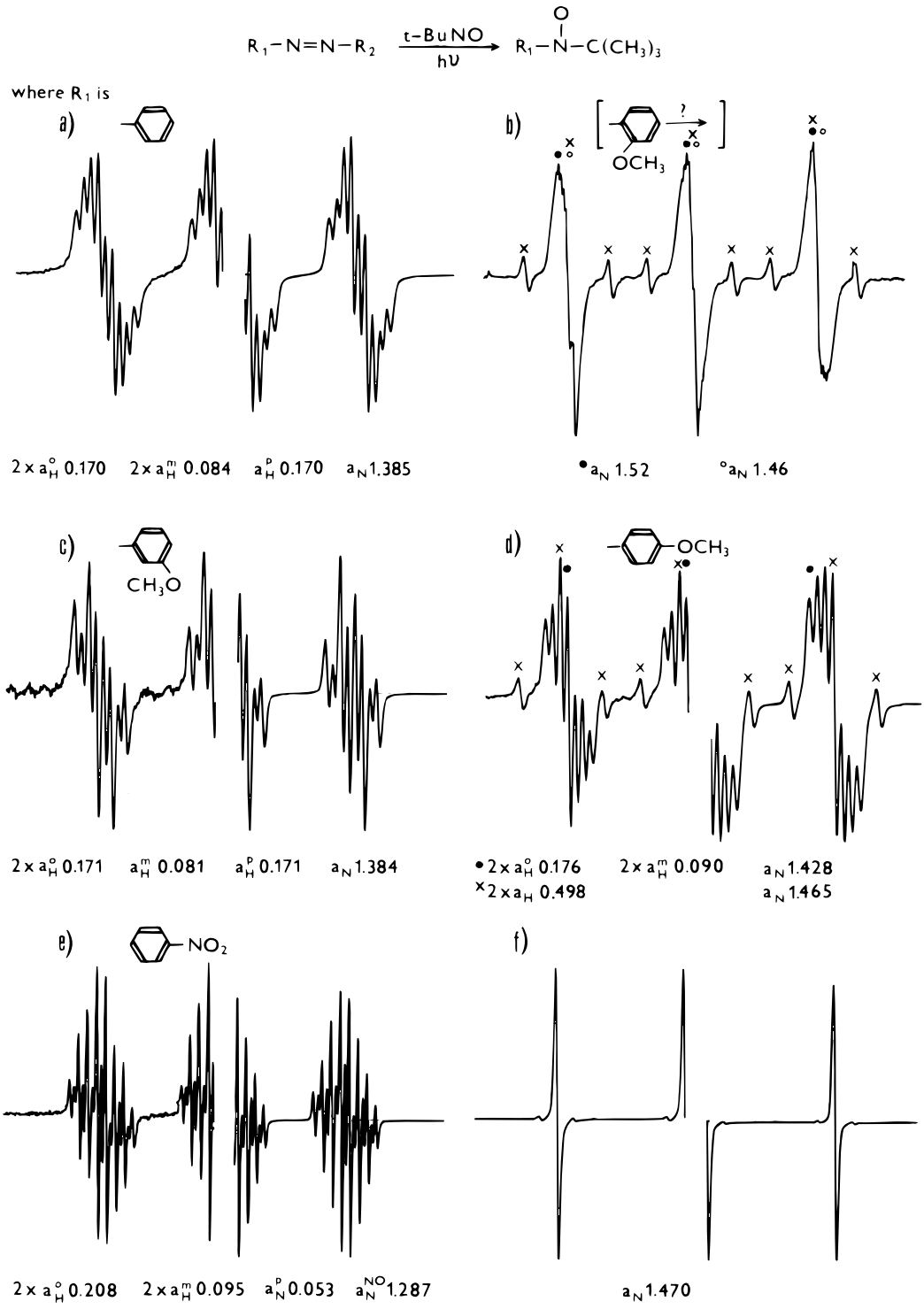

Figure 2. Experimental (left) and simulated (right) EPR spectra with splitting constants (mT) of ^{t}BuNO adducts observed during the photochemical decomposition of azo compounds (a) **IVa**, (b) **IVc**, (c) **IVd**, (d) **IVe**, (e) **XI** and (f) **IVa**, **e**, and **j**. In (b) only the experimental spectrum is shown.

abstract hydrogen from the neighboring molecules or dimerize to ^{1}R—^{2}R products. These decomposition products can be further reduced as described below.

Stable radicals. Stable anion radicals, generated by the *in situ* cathodic reduction in the region of the first reduction step directly in the cavity of an EPR spectrometer, were observed for azophosphonates (**III**), azosulfonates (**IV**), azosulfones (**V**) and acyl- and diacylazo compounds (**X**). The splitting constants extracted by the simulation from the experimental EPR spectra are summarized in Table 3. The EPR spectra are relatively complex, owing to the numerous nuclei contributing to the hyperfine structure, as is demonstrated in Fig. 6 using compounds **IVa** and **IVb**. The assignment of splitting constants to the individual nuclei was based on the

Table 1. EPR parameters of spin trap adducts formed from compounds containing azo groups (**I–XII**) on UV irradiation (UV), cathodic reduction ($+e^-$) and thermal decomposition (T)

Type	Spin trap	Solvent	Experiment		a_N(NO)	Splitting constants (mT) a_H	*g*-Factor	Ref.
(1) $^{\cdot}C_6H_5$	DMPO	H_2O	**IVa**	UV	1.54	2.46	2.0059	21
		MeOH	**IVa, Va**	UV	1.50	2.22	2.0059	21
		EtOH	**IVa, Va**	UV	1.49	2.16	2.0059	21
		C_6H_6	**Va**	UV	1.395	1.985	2.0059	21
		PrOH	**IVa**	UV	1.509	2.14	2.0059	21
	ND	CH_3CN	**IVa, VIIIa**	UV	1.050	$^{p,o,o}3 \times 0.287$, $^{m,m}2 \times 0.097$	2.0057	22, 32
			Xa–c	UV	1.055	$^{p}0.292$, $^{o,o}2 \times 0.281$, $^{m,m}2 \times 0.095$	2.0057	32
			IIa, i, m	UV	1.022	$^{p}0.28$, $^{o,o}2 \times 0.279$, $^{m,m}2 \times 0.097$	2.0057	32
	^{t}BuNO	MeOH	**IVa**	UV	1.385	$^{p,o,o}3 \times 0.17$, $^{m,m}2 \times 0.084$	2.0058	22
(2) $^{\cdot}C_6H_4$ $_{o}CH_3O$	DMPO	H_2O	**IVc**	UV	1.59	2.407	2.0059	21
		MeOH	**IVc**	UV	1.50	2.14	2.0059	21
		EtOH	**IVc**	UV	1.509	2.14	2.0059	21
	^{t}BuNO	MeOH	**IVc**	UV	1.52	Low unresolved splittings	2.0058	22
(3) $^{\cdot}C_6H_4$ $_{m}CH_3O$	DMPO	H_2O	**IVd**	UV	1.587	2.43	2.0056	21
		MeOH	**IVd**	UV	1.494	2.17	2.0058	21
		EtOH	**IVd**	UV	1.486	2.124	2.0057	21
	ND	CH_3CN	**IVd**	UV	1.04	$^{p,o,o}3 \times 0.281$, $^{m}0.09$	2.0056	22
	^{t}BuNO	MeOH	**IVd**	UV	1.384	$^{p,o,o}3 \times 0.171$, $^{m}0.081$	2.0058	22
(4) $^{\cdot}C_6H_4$ $_{p}CH_3O$	DMPO	H_2O	**IVe**	UV	1.592	2.495	2.0058	21
		MeOH	**IVe**	UV	1.514	2.246	2.0058	21
		EtOH	**IVe**	UV	1.50	2.20	2.0058	21
	^{t}BuNO	MeOH	**IVe**	UV	1.428	$^{o,o}2 \times 0.176$, $^{m,m}2 \times 0.09$	2.0057	22
	ND	CH_3CN	**VIIn**	UV	1.09	$^{o,o}2 \times 0.285$, $^{m,m}0.088$, $^{p\text{-}CH_3O}3 \times 0.037$	2.0057	32
(5) $^{\cdot}C_6H_4$ $_{m}CH_3$	DMPO	MeOH	**Vb**	UV	1.50	2.22	2.0058	21
		EtOH	**Vb**	UV	1.48	2.16	2.0058	21
		C_6H_6	**Vb**	UV	1.395	1.975	2.0058	21
		$C_6H_5CH_3$	**Vb**	UV	1.392	1.955	2.0058	21
	ND	CH_2Cl_2	**Vb**	UV	1.066	$^{p,o,o}3 \times 0.291$, $^{m,m\text{-}CH_3}4 \times 0.099$	2.0055	22
(6) $^{\cdot}C_6H_4$ $_{p}CH_3$	DMPO	MeOH	**Vc**	UV	1.50	2.22	2.0059	21
		EtOH	**Vc**	UV	1.49	2.18	2.0059	21
		C_6H_6	**Vc**	UV	1.40	1.99	2.0059	21
		$C_6H_5CH_3$	**Vc**	UV	1.392	1.995	2.0059	21
(7) $^{\cdot}C_6H_4$ $_{p}Cl$	DMPO	MeOH	**Vd**	UV	1.49	2.19	2.0060	21
		EtOH	**Vd**	UV	1.49	2.195	2.0060	21
		C_6H_6	**Vd**	UV	1.387	2.026	2.0060	21
		$C_6H_5CH_3$	**Vd**	UV	1.375	1.965	2.0060	21
	ND	CH_3CN	**IXa, b**	UV, T	0.993	$^{o,o}2 \times 0.276$, $^{m,m}2 \times 0.098$, $^{p\text{Cl}}0.03$	2.0058	25
	^{t}BuNO	CH_3CN	**IXa, b**	$+e^-$	1.25	$^{o,o}2 \times 0.287$, $^{m,m}2 \times 0.1$, $^{p\text{Cl}}0.031$	2.0058	25

(8) $^{\cdot}C_6H_{3\ o,oCl_2}$	DMPO	H_2O	**IIg**	UV	1.504	2.124	2.0060	21
		EtOH	**IIg**	UV	1.501	2.22	2.0060	21
		CCl_4	**IIg**	UV	1.38	2.19	2.0060	21
		$CHCl_3$	**IIg**	UV	1.36	1.93	2.0060	21
		C_6H_6	**IIg**	UV	1.335	1.90	2.0060	21
		$C_6H_5CH_3$	**IIg**	UV	1.357	1.903	2.0060	21
(9) $^{\cdot}C_6H_{4\ p\mathrm{Br}}$	DMPO	MeOH	**IIh**	UV	1.50	2.19	2.0060	21
		EtOH	**IIh**	UV	1.504	2.205	2.0060	21
		CCl_4	**IIh**	UV	1.392	1.95	2.0060	21
		$CHCl_3$	**IIh**	UV	1.45	2.06	2.0060	21
		C_6H_6	**IIh**	UV	1.39	1.95	2.0060	21
		$C_6H_5CH_3$	**IIh**	UV	1.39	1.96	2.0060	21
(10) $^{\cdot}C_6H_{4\ p\mathrm{NO_2}}$	DMPO	MeOH	**IIf, Ve**	UV	1.485	2.16	2.0059	21
		EtOH	**IIf, Ve**	UV	1.48	2.115	2.0059	21
		CCl_4	**IIf**	UV	1.38	1.96	2.0059	21
		$CHCl_3$	**IIf**	UV	1.43	2.03	2.0059	21
		C_6H_6	**IIf**	UV	1.37	1.95	2.0059	21
		$C_6H_5CH_3$	**IIf**	UV	1.37	1.955	2.0059	21
	ND	CH_2Cl	**IIf, Ve**	UV	0.906 $^{p\mathrm{NO_2}}$0.074	^{o,o}2 × 0.269, ^{m,m}2 × 0.096	2.0059	22
		CH_3CN	**IIb, VIIIe**	UV	0.92 $^{p\mathrm{NO_2}}$0.074	^{o,o}2 × 0.263, ^{m,m}2 × 0.1		32
	^{t}BuNO	H_2O	**XI**	UV	1.287 $^{p\mathrm{NO_2}}$0.053	^{o,o}2 × 0.208, ^{m,m}2 × 0.095	2.0058	22
		C_6H_6	**IIf, Ve**	UV	1.046 $^{p\mathrm{NO_2}}$0.056	^{o,o}2 × 0.223, ^{m,m}2 × 0.09	2.0059	22
		CH_2Cl_2	**XI**	$+e^-$	1.08 $^{p\mathrm{NO_2}}$0.057	^{o,o}2 × 0.223, ^{m,m}2 × 0.092		29
(11) $^{\cdot}C_6H_{4\ p\mathrm{NH_2}}$	DMPO	H_2O	**IVj**	UV	1.611	2.505		22
		MeOH	**IVj**	UV	1.533	2.231		22
		EtOH	**INj**	UV	1.505	2.207		22
(12) $^{\cdot}C_6H_{4\ p\mathrm{OH}}$	DMPO	H_2O	**IVi**	UV	1.616	2.490		22
		MeOH	**IVi**	UV	1.479	2.173		22
		EtOH	**IVi**	UV	1.509	2.207		22
(13) $^{\cdot}C_6H_{4\ p\mathrm{COOH}}$	DMPO	H_2O	**VIIh**	UV	1.587	2.446		22
		MeOH	**IIi**	UV	1.513	2.162		22
	ND	CH_3CN	**IIi**	UV	0.967	^{o,o}2 × 0.275, ^{m,m}2 × 0.099	2.0061	22
(14) $^{\cdot}C_6H_{4\ m\mathrm{COOH}}$	DMPO	CH_3CN	**VIIa–d**	UV	1.495	2.175	2.0058	24
	ND	CH_3CN	**VIIa–d, VId**	UV	1.076	^{p}0.306, ^{o,o}2 × 0.285, ^{m}0.096	2.0057	24, 30
(15) $^{\cdot}C_6H_{3\ m,m(\mathrm{COOH})_2}$	DMPO	H_2O	**IVf**	UV	1.572	2.402		22
		MeOH	**IVf**	UV	1.484	2.173		22

Table 1. Continued

Type	Spin trap	Solvent	Experiment		a_N(NO)	Splitting constants (mT) a_H	g-Factor	Ref.
		EtOH	**IVf**	UV	1.484	2.173		22
	ND	CH_3CN	**VIIe, f**	UV	1.054	^{p}0.295, ^{o,o}2 × 0.275		24
			VIe	UV	1.054	^{p}0.295, ^{o,o}2 × 0.275	2.0057	30
(16) $^{\cdot}C_6H_{3\ m,m(COOCH_3)_2}$	DMPO	H_2O	**IVg**	UV	1.548	2.334		22
		MeOH	**IVg**	UV	1.494	2.139		22
		EtOH	**IVg**	UV	1.509	2.187		22
	ND	CH_3CN	**IVg**	UV	0.996	^{p,o,o}3 × 0.279	2.0057	22
(17) $^{\cdot}C_6H_{3\ p\mathrm{OH},o\text{-}X}$	^{t}BuNO	H_2O	**IVi**	UV	1.516	^{o}0.212, ^{m,m}2 × 0.085	2.0059	22
(18) $^{\cdot}C_6H_{4\ pR_1}$	ND	CH_3CN	**IIXc, d**	UV, T	0.967	^{o,o}2 × 0.278, ^{m,m}2 × 0.097	2.0058	25
			VIIm	T	1.065	^{o,o}2 × 0.274, ^{m,m}2 × 0.087	2.0057	32
			VIIn	T	1.066	^{o,o}2 × 0.274, ^{m,m}2 × 0.093	2.0057	32
	^{t}BuNO	MeOH	**IXc, d**	$+e^-$	1.272	^{o,o}2 × 0.272, ^{m,m}2 × 0.096	2.0058	25
(19) $^{\cdot}C_6H_{4\ pSO_3H}$	ND	CH_3CN	**VIf**	UV	1.030	^{o,o}2 × 0.283, ^{m,m}2 × 0.106	2.0059	30
(20) $^{\cdot}C_6H_{4\ mSO_2R}$	ND	CH_3CN	**VIj**	$+e^-$	0.999	^{p}0.285, ^{o,o}2 × 0.28, ^{m}0.093	2.0057	30
(21) $^{\cdot}C_6H_{4\ pCOR}$	ND	CH_3CN	**VIh**	$+e^-$	0.966	^{o,o}2 × 0.277, ^{m,m}2 × 0.101	2.0057	30
(22) $^{\cdot}C_6H_{4\ pCOONa}$	ND	CH_3CN	**VIIk, I**	UV	0.807	^{o}0.289, $_{o}$0.26, ^{m}0.09, ^{m}0.085	2.0057	32
(23) $^{\cdot}C_6H_{4\ pCH_2OH}$	ND	C_6H_6	**IIj**	T	1.025	^{pCH_2}2 × 0.278, ^{o,o}2 × 0.278, ^{m,m}2 × 0.095		33
(24) $^{\cdot}SO_3Na$	DMPO	H_2O	**IVa–e**	UV	1.45	1.6	2.0058	21
			IVf, g, i, j	UV	1.46	1.626		22
		MeOH	**IVa–e**	UV	1.40	1.49	2.0058	21
			IVg, j	UV	1.365	1.49		22
		EtOH	**IVa–e**	UV	1.41	1.51	2.0058	21
			IVi	UV	1.372	1.465		22
	^{t}BuNO	H_2O	**IVa, e, j**	UV	1.47		2.0055	22
		MeOH	**IVc**	UV	1.46		2.0056	22
(25) $^{\cdot}SO_2C_6H_5$	DMPO	$CHCl_3$	**Va–d**	UV	1.37	1.60	2.0062	21
		C_6H_6	**Va–d**	UV	1.26	1.31	2.0062	21
		$C_6H_5CH_3$	**Va–d**	UV	1.255	1.31	2.0062	21
	ND	CH_2Cl_2	**Vb**	UV	1.12		2.0062	22
(26) $^{\cdot}C(CH_3)_3$	^{t}BuNO	H_2O	^{t}BuNO	UV	1.72		2.0058	22
		MeOH	^{t}BuNO	UV	1.62		2.0058	22
(27) $^{\cdot}CR^1R^2R^3$	DMPO	CH_3CN	**Ia, b**	UV	1.511	2.177		32
		H_2O	**If**	UV	1.543	2.475		22
			Ig	UV	1.548	2.461		22
			Ii	UV	1.558	2.480		22
		MeOH	**Il**	UV	1.513	2.135		22
			Ig	UV	1.459	2.378		22
			Ii	UV	1.513	2.378		22
	ND	C_6H_6	**Ia**	UV, T	1.412		2.0057	32
			Ib	UV	1.347		2.0057	32

(28) $^{\cdot}C$	DMPO	CH_3CN	**IXa–d**	UV	1.398	2.120	2.0059	25
			VIa–j	UV	1.484	2.182	2.0057	30
			VIIIa–e	UV	1.435	2.125		26
			VIIk, l, n	UV	1.45	2.16	2.0057	32
(29) $^{\cdot}CH_2CN$	ND	CH_3CN	**VIIj**	UV	1.342	2 × 0.977		28
			VIa–f	UV	1.343	2 × 0.977	2.0059	30
			Xa–c	UV	1.355	2 × 0.97	2.0059	32
			VIIIa–e	UV	1.345	2 × 0.97		26
			IXa–d	UV	1.39	2 × 0.946	2.0059	25
			VIIk, l, n	UV	1.35	2 × 0.982	2.0057	32
(30) $^{\cdot}COCH_3X$	^{t}BuNO	MeOH	**IVc, e**	UV	1.465	0.996, 2 × 0.498	2.0056	22
(31) $^{\cdot}CH(X)$	ND	CH_3CN	**VIIIa**	UV	1.3	0.6		26
(32) $^{\cdot}CH_3$	ND	CH_3CN	**IXb–d**	UV	1.41	3 × 1.277	2.0060	25
(33) $^{\cdot}C_{HX(CH_2)_2CH_3}$	^{t}BuNO	CH_3CN	**IXa–d**	$+e^-$	1.478	0.21, 2 × 0.03	2.0057	25
			IIa, c, l	$+e^-$	1.48	0.19, 2 × 0.044	2.0057	32
(34) $^{\cdot}CH_2CH_3$	ND	CH_3CN	**VIIIa–c**	UV	1.395	2 × 1.184		26
(35) $^{\cdot}COR$	DMPO	CH_3CN	**Xa–c**	UV	1.418	2.62	2.0061	32
	ND	CH_3CN	**Xd–f**	UV	0.729		2.0060	32
(36) $^{\cdot}C(CN)_2CH_3$	ND	CH_3CN	**IIa–e**	UV	1.309		2.0057	32
(37) $^{\cdot}OH$	DMPO	H_2O	**Ie**	UV	1.401	1.401		22
			If	UV	1.421	1.421		22
			Ig	UV	1.450	1.450		22
		MeOH	**Ii**	UV	1.405	1.405		22
(38) $^{\cdot}?OCH_3$	DMPO	CH_3CN	**VIIIc**	UV	1.338	0.796, 0.165		26
(39) $^{\cdot}O_{n\ CR^1CH_3CN}$	DMPO	C_6H_6	**Id**	UV	1.265	0.806, 0.18		22
			Ij	UV	1.33	0.845		22
			Ih	UV	1.298	0.835		22
			IIi	UV	1.26	0.8		22
			Ik	UV	1.357	0.966		22
		MeOH	**Ik**	UV	1.405	0.97		22
			Ij	UV	1.351	0.97		22
(40) $^{\cdot}O_{n\ CR^1(CH_3)_2}$	DMPO	C_6H_6	**Ie**	UV	1.275	0.771		22
			Il	UV	1.324	0.918		22
(41) $^{\cdot}O_{n\ C(CH_3)_2CN}$	DMPO	C_6H_6	**Ic**	UV	1.264	0.842, 0.185, 0.067		22
(42) $^{\cdot}O_{n\ C(CH_3)_3}$	DMPO	C_6H_6	TBHP	UV	1.3	0.942, 0.168		22
(43) $^{\cdot}O_{n\ C(CH_3)_3}$	DMPO	C_6H_6	^{t}BuOO-CoL_2OH		1.3	0.8, 0.19		22
				UV				
(44) $^{\cdot}O_{n\ (CH_3)_2C_6H_6}$	DMPO	C_6H_6	Cumyl-OOH	UV	1.355	1.015, 0.145		22

Table 1. Continued

Type	Spin trap	Solvent	Experiment		Splitting constants (mT) a_N(NO)	a_H	*g*-Factor	Ref.
(45) $^{\cdot}NX_1X_2$	DMPO	CH_3CN	**VIIg**	UV	1.45	2.0		24
					0.23			
			Xd	UV	1.284	1.08	2.0064	32
					0.078			
			Xe, f	UV	1.376	1.73	2.0067	32
					0.33			
(46) $^{\cdot}SC_6H_4R$	ND	CH_3CN	**VIa–j**	UV, $+e^-$	1.63		2.0065	30
(47) $^{\cdot}SR$	DMPO	CH_3CN	**VIa–j**	UV	1.340	1.482	2.0060	30
(48) $^{\cdot}H$	ND	C_6H_6	**IXa–d**	T	1.426	1.367	2.0059	25
$^{\cdot}D$	ND	C_6D_6	**IXa–d**	T	1.426	D: 0.21	2.0059	25
(49) $^{\cdot}X_1$	DMPO	H_2O	**IVa**	UV	1.44		2.0058	21
		MeOH	**IVa, d**	UV	1.44		2.0058	21
		EtOH	**IVd**	UV	1.42		2.0058	21
(50) $^{\cdot}X_2$	DMPO	H_2O	**IVc**	UV	1.665	2.84	2.0056	21
(51) $^{\cdot}X(H)$	ND	CH_3CN	**VIIIa–c**	UV	1.343	0.84		26
Free radicals								
(52) $^{\cdot}CCN(CH_3)_2$		C_6H_6	**Ic**	UV	0.34	6×2.065		53a
(53) $^{\cdot}C(CN)CH_3CH_2$	COONa	$H_2O_{(NaHCO_3)}$	**Ill**	UV	0.35	5×2.12		27
(54) $^{\cdot}C(Ph)_3$		$C_6H_5CH_3$	**IIn**	T		Singlet		53b
(55) $^{\cdot}SO_3Na$		EtOH	**IVa–e**	UV		Singlet		23
(56) $^{\cdot}NOPhX$		CH_3CN	**VIIg**	UV	1.29	$^{p}0.42$, $^{o,o}2 \times 0.36$	2.0057	24

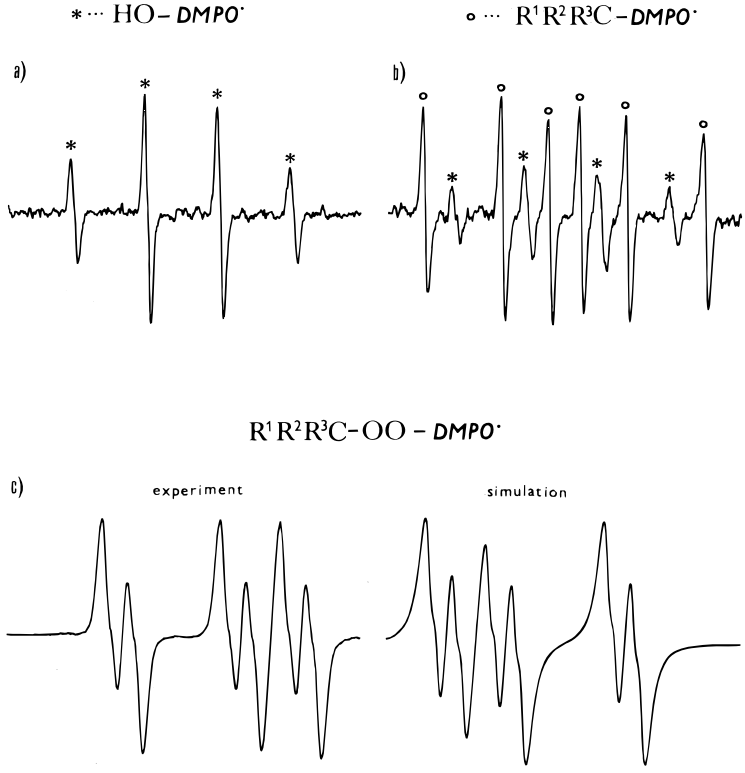

Figure 3. EPR spectra of DMPO adducts observed during the photochemical decomposition of azo compounds (a) **Id** during the first minute of irradiation in water, (b) **If** after 5 min of irradiation in water and (c) **Ic**, experimental (lower half of field) and simulated (upper half of field) spectra in benzene (a_N and a_H are splitting constants in mT).

generally known distribution of the unpaired spin density on the phenyl ring. In this case the smallest splitting constants were assigned to the *meta*, the next two higher splittings to the *ortho* and the still higher splitting constant to the *para* proton. Additionally, this was unambiguously confirmed by our further experiments, since upon replacing the *meta*, *ortho* or *para* hydrogens with, e.g., methoxy, methyl or chlorine the corresponding hydrogen splitting constants were eliminated (see Table 3). The distribution of the spin density on the phenyl ring clearly indicates a π-character of the corresponding anion radicals. A variable non-equivalence of the *ortho* and *meta* protons points to varying degrees of hindered rotation of the phenyl ring around the azo group.

The assignment of nitrogen splitting constants was based on the $^{15}N^{1}$ substitution as shown in Fig. 6(b). The EPR spectrum of [^{15}N]**IVb** anion radical was simulated, replacing the nitrogen splitting constant $a_{14N} = 0.589$ mT with $a_{15N} = 0.832$ mT, taking into account also the change in nuclear spin from $I = 1$ to $I = \frac{1}{2}$. Consequently, the lower nitrogen splitting was assigned to the nitrogen attached to the phenyl group. The relatively small difference between the nitrogen splittings for azosulfonates (**IV**) became larger in azosulfones (**V**) and azophosphonates (**III**) owing to the stronger acceptor properties of —SO_2—Ph and —PO—OCH_3 groups. In symmetric diacylazo compounds (**Xd–f**) equal nitrogen splittings were found, similarly to those already published for other symmetric azo compounds.[49–52] The characteristic g-values for anion radicals of the azo compounds are $g \approx 2.0040 \pm 0.0001$. They are slightly higher (2.0044 ± 0.0001) in azo compounds with nitro- and chlorine-substituted phenyl rings. Still higher g-values (2.0050–2.0060) were observed for nitro group-centered anion radicals and anion radicals of diacylazo compounds.

Unstable radicals. From all 1-aryl-2-alkylazo compounds (**II**) only the nitro-substituted derivatives **IIb, d** and **f** form relatively stable anion radicals in the potential region of the first reduction step, as illustrated with the EPR spectrum in Fig. 7(a) using compound **IIf**. Its complete simulation was ambiguous but the g-value (2.0052), the spectral width and a few splitting constants extracted from a partial analysis correspond well to the expected parameters of anion radical [**IIf**]$^{-\cdot}$. At the higher potential the anion radical decomposed and formed a cage product, which was then reduced to the anion radical centered on its nitro group, as illustrated in Fig. 7(b). At still higher potentials a new nitro-centered anion radical pX-$C_6H_4NO_2^{-\cdot}$ was found [Fig. 7(c)] with X possibly as —NH_2 or —N=CH_2, indicating a complex reaction of non-stable radicals produced in this potential region. A similar formation of cage products at the higher reduction potentials was observed also in the case of other azo compounds (e.g. **IIb** and **d**). Their original anion radicals are not stable.

In order to prove the formation of $^{1}R^{\cdot}$ and $^{2}R^{\cdot}$ radicals in the cathodically initiated decomposition of azo compounds, ^{t}BuNO and ND spin traps were used, and

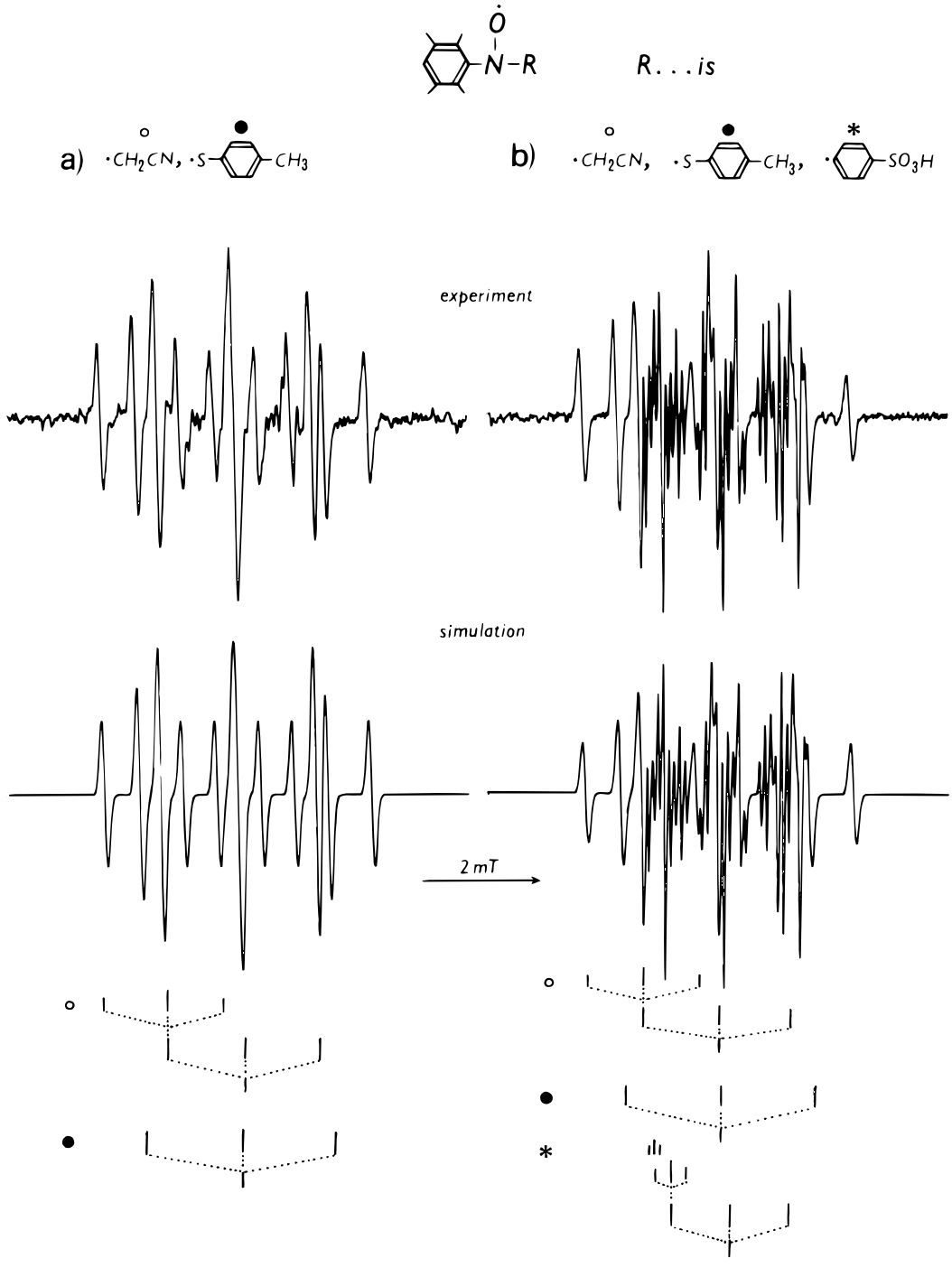

Figure 4. EPR spectra of ND adducts observed during the photochemical decomposition of azosulfides (a) **VIa–c** and (b) **VIf** in acetonitrile.

usually two types of radicals were found. The radical products of a direct splitting of the azo group-containing compounds are mostly represented by the corresponding substituted phenyl groups trapped to ^{t}BuNO. The second type of radicals $^{\cdot}$CHXR observed in the cathodic reduction of **IIa**, **c**, **l** and **IX** consists of secondary products and originates from the support electrolyte (TBAP). They are formed after H abstraction from electrolyte to the $^{1}R^{\cdot}$ and $^{2}R^{\cdot}$, which represent the primary products of azo compounds decomposition. That was clearly demonstrated by the reduction of diazonium salt **XI**, where the nitrobenzene anion radical was observed. The expected *p*-nitrophenyl radical intermediate was confirmed by ^{t}BuNO spin trap. The abstraction of hydrogen from the support electrolyte (e.g. 0.1 M TBAP in dichloromethane) to the *p*-nitrophenyl radical was verified using deuterated dichloromethane (CD_2Cl_2). The EPR spectrum observed in the cathodic reduction of **XI** in CD_2Cl_2 was successfully simulated as the sum of two different *p*-

Table 2. EPR parameters of hydrazyl radicals photochemically generated from compounds **IV** and **Xd–f**

Type (hydrazyl radicals)	Experiment	Splitting constants (mT)		*g*-Factor	Ref.
		a_{N2}, a_{N1}	a_H		
(91) C_6H_5—N(SO_3Na)—N˙—SO_3Na	**IVa** (H_2O, 275 K)	1.125, 1.024	$^{o,o}2 \times 0.063$, $^{m,m}2 \times 0.061$, $^{p}0.032$	2.0037	23
(92) C_6H_5—^{15}N(SO_3Na)—N˙—SO_3Na	**IVb** (H_2O, 275 K)	1.125, ^{15}N:1.44	$^{o,o}2 \times 0.063$, $^{m,m}2 \times 0.061$, $^{p}0.032$	2.0037	23
(93) $_{o}CH_3OC_6H_4$—N(SO_3Na)—N˙—SO_3Na	**IVc** (H_2O, 275 K)	1.125, 1.05	$^{o,m,m}3 \times 0.064$, $^{p} < 0.02$	2.0037	23
(94) $_{m}CH_3OC_6H_4$—N(SO_3Na)—N˙—SO_3Na	**IVd** (H_2O, 275 K)	1.115, 1.028	$^{o,o,m}3 \times 0.064$, $^{p}0.029$	2.0038	23
(95) $_{p}CH_3OC_6H_4$—N(SO_3Na)—N˙—SO_3Na	**IVe** (H_2O, 275 K)	1.12, 1.028	Low stability, poor resolution		23
(96) C_6H_5—N(H*)—N˙—SO_3Na	**IVa** (EtOH, 320 K)	0.976, 0.738	$^{H*}0.805$, $^{p}0.25$, $^{o}0.24$, $^{o}0.23$, $^{m,m}2 \times 0.077$	2.0037	23
(97) C_6H_5—^{15}N(H*)—N˙—SO_3Na	**IVb** (EtOH, 320 K)	0.976, ^{15}N:1.032	$^{H*}0.805$, $^{p}0.25$, $^{o}0.24$, $^{o}0.23$, $^{m,m}2 \times 0.077$	2.0037	23
(98) C_6H_5—N(D*)—N˙—SO_3Na	**IVa** (EtOD, 320 K)	0.976, 0.738	$^{D*}0.123$, $^{p}0.25$, $^{o}0.24$, $^{o}0.23$, $^{m,m}2 \times 0.077$	2.0037	23
(99) $_{o}CH_3OC_6H_4$—N(H*)—N˙—SO_3Na	**IVc** (EtOH, 320 K)	0.965, 0.715	$^{H*}0.80$, $^{p}0.274$, $^{o}0.264$, $^{m,m}2 \times 0.073$	2.0038	23
(100) $_{m}CH_3OC_6H_4$—N(H*)—N˙—SO_3Na	**IVd** (EtOH, 320 K)	0.965, 0.731	$^{H*}0.797$, $^{p}0.247$, $^{o}0.238$, $^{o}0.228$, $^{m}0.078$	2.0036	23
(101) [C_6H_5—CO]$_2$N—N˙—COC_6H_5	**Xd** (MeCN, C_6H_6)	1.02, 0.518		2.0049	32
(102) [$_{p}ClC_6H_4$—CO]$_2$N—N˙—$COC_6H_{4p}Cl$	**Xe** (MeCN, C_6H_6)	0.978, 0.525		2.0051	32
(103) [$_{p}CH_3C_6H_4$—CO]$_2$N—N˙—$COC_6H_{4p}CH_3$	**Xf** (MeCN, C_6H_6)	1.027, 0.521		2.0048	32

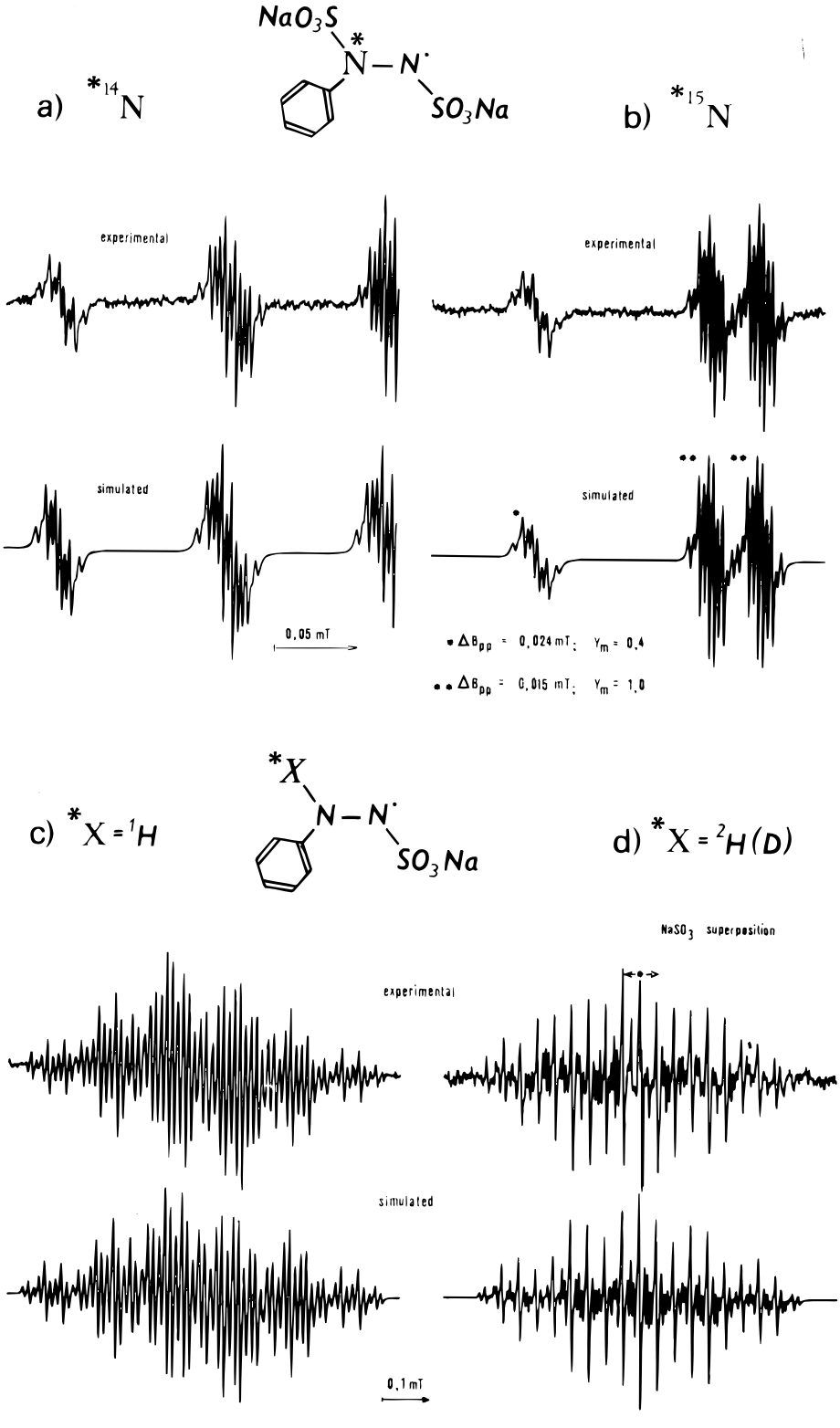

Figure 5. The left half of the EPR spectra observed at 275 K in the photochemical decomposition of (a) **IVa** and (b) **IVb** in water (identical spectra were found in D_2O and in H_2O). ΔB = peak-to-peak width; Y_m = maximum difference between line amplitudes. EPR spectra obtained at 320 K in the photochemical decomposition of **IVa** in (c) EtOH and (d) EtOD.

Table 3. EPR parameters of anion radicals cathodically generated in 0.1 M TBAP acetonitrile solutions from compounds **II–V** and **X**

Type (anion radicals)	Substrate	Splitting constants (mT)		*g*-Factor	Ref.
		a_{N^1}, a_{N^2}	a_H		
(57) $[C_6H_5-N=N-SO_3Na]^{-\cdot}$	**IVa**	0.5892, 0.618	^{p}0.378, ^{o}0.3505, ^{o}0.248, ^{m}0.107, ^{m}0.0735	2.0040	29
(58) $[C_6H_5-{}^{15}N=N-SO_3Na]^{-\cdot}$	**IVb**	^{15}N:0.832, 0.6185	^{p}0.378, ^{o}0.3505, ^{o}0.248, ^{m}0.107, ^{m}0.0735	2.0040	29
(59) $[{}^{o}CH_3OC_6H_4-N=N-CO_3Na]^{-\cdot}$	**IVc**	0.58, 0.5885	$^{p,o}2 \times 0.3931$, ^{m}0.1135, ^{m}0.0535	2.0040	29
(60) $[{}^{m}CH_3OC_6H_4-N=N-SO_3Na]^{-\cdot}$	**IVd**	0.59, 0.6	^{p}0.389, ^{o}0.3325, ^{o}0.252, ^{m}0.074	2.0040	29
(61) $[{}^{p}CH_3OC_6H_4-N=N-SO_3Na]^{-\cdot}$	**IVe**	0.5762, 0.641	^{o}0.3815, ^{o}0.2547, $^{m,m}2 \times 0.098$, $^{p\mathrm{CH_3O}}3 \times 0.0293$	2.0040	29
(62) $[{}^{m,m(COOCH_3)_2}C_6H_3N=NSO_3Na]^{-\cdot}$	**IVf**	0.47, 0.636	^{p}0.442, $^{o,o}2 \times 0.184$	2.0039	29
(63) $[{}^{m,m(COOH)_2}C_6H_3-N=N-SO_3Na]^{-\cdot}$	**IVg**	0.58, 0.686	^{p}0.375, ^{o}0.36, ^{o}0.2515	2.0041	29
(64) $[C_6H_4-N=N-SO_2-C_6H_5]^{-\cdot}$	**Va**	0.8691, 0.362	^{p}0.4055, ^{o}0.384, ^{o}0.33, $^{m,m}2 \times 0.1196$	2.0041	29
(65) $[{}^{m}CH_3C_6H_4-N=N-SO_2-C_6H_5]^{-\cdot}$	**Vb**	0.8685, 0.334	^{p}0.4065, ^{o}0.378, ^{o}0.334, $^{m,m\mathrm{CH_3}}4 \times 0.116$	2.0041	29
(66) $[{}^{p}CH_3C_6H_4-N=N-SO_2-C_6H_5]^{-\cdot}$	**Vc**	0.8648, 0.3751	$^{p\mathrm{CH_3}}3 \times 0.4348$, $^{o,o}2 \times 0.369$, $^{m,m}2 \times 0.123$	2.0041	29
(67) $[{}^{p}ClC_6H_4-N=N-SO_2-C_6H_5]^{-\cdot}$	**Vd**	0.832, 0.3805	^{o}0.3825, ^{o}0.3225, $^{m,m}2 \times 0.126$, $^{p\mathrm{Cl}}$0.019	2.0044	29
(68) $[{}^{p}NO_2C_6H_4-N=N-SO_2-C_6H_5]^{-\cdot}$	**Ve**	0.556, 0.455, $^{p\mathrm{NO_2}}$0.032	^{o}0.3, ^{o}0.239, $^{m,m}2 \times 0.09$	2.0043	29
(69) $[{}^{p}NO_2C_6H_4-N=N-C(CH_2)CN]^{-\cdot}$	**IIb**		Simulation ambiguous		29
(70) $[NO_2C_6H_4-C(CH_3)_2CN]^{-\cdot}$	**IIb**	$^{\mathrm{NO_2}}$1.0225	$^{o,o}2 \times 0.335$, $^{m,m}2 \times 0.108$	2.0052	29
(71) $[NO_2C_6H_5]^{-\cdot}$	**XI**$_{CH_2Cl_2}$	$^{\mathrm{NO_2}}$1.0645	^{p}0.3835, $^{o,o}2 \times 0.3325$, $_{m,m}2 \times 0.1075$	2.0051	29
$[NO_2C_6H_4D]^{-\cdot}$	**XI**$_{CD_2Cl_2}$	$^{\mathrm{NO_2}}$1.0815	$^{p\mathrm{D}}$0.0587, $^{o,o}2 \times 0.3325$, $^{m,m}2 \times 0.1075$	2.0051	29
$[NO_2C_6H_5]^{-\cdot}$	**VIa**	$^{\mathrm{NO_2}}$1.042	^{p}0.369, $^{o,o}2 \times 0.336$, $^{m,m}2 \times 108$	2.0045	30
(72) $[NO_2C_6H_4X]^{-\cdot}$	**IIb**	$^{\mathrm{NO_2}}$1.221, $^{p\mathrm{N}}$0.11	$^{o,o}2 \times 0.34$, $^{m,m}2 \times 0.11$, $^{p\mathrm{H}}2 \times 0.09$		29
(73) $[NO_2C_6H_4-SO_2-C_6H_5]^{-\cdot}$	**Ve**	$^{\mathrm{NO_2}}$1.3906	$^{o,o}2 \times 0.3086$, $^{m,m}2 \times 0.0742$		29
(74) $[NO_2C_6H_4pR]^{-\cdot}$	**VIa**	$^{\mathrm{NO_2}}$0.782	^{o}0.372, ^{o}0.287, ^{m}0.124, ^{m}0.09	2.0065	30
(75) $[NO_2C_6H_4mR]^{-\cdot}$	**VIb**	$^{\mathrm{NO_2}}$0.996	^{p}0.402, $^{o,o}2 \times 0.335$, ^{m}0.105	2.0045	30
(76) $[X-C_6H_4-NY]^{-\cdot}$	**Xd**	1.184	$^{o,o}2 \times 0.328$, $^{m,m}2 \times 0.115$	2.0051	32
(77) $[NO_2-C_6H_4oR]^{-\cdot}$	**IId**	0.966	^{p}0.416, ^{o}0.336, $^{m,m}2 \times 0.111$	2.0051	32
(78) $[C_6H_5NR]^{-\cdot}$	**IIi**	1.128	^{p}0.404, $^{o,o}2 \times 0.346$, $^{m,m}2 \times 0.111$	2.0051	32
(79) $[C_6H_5-N=N-PO(OCH_3)_2]^{-\cdot}$	**IIIa**	0.83, 0.37	^{p}0.415, ^{o}0.38, ^{o}0.31, ^{m}0.125, ^{m}0.11, P:0.9	2.0040	31
(80) $[C_6H_5-{}^{15}N=N-PO(OCH_3)_2]^{-\cdot}$	**IIIb**	^{15}N:1.167, 0.37	^{p}0.415, ^{o}0.38, ^{o}0.31, ^{m}0.125, ^{m}0.11, P:0.9	2.0040	31
(81) $[{}^{p}ClC_6H_4-N=N-PO(OCH_3)_2]^{-\cdot}$	**IIIc**	0.812, 0.373	^{o}0.383, ^{o}0.31, $^{m,m}2 \times 0.117$, $^{p\mathrm{Cl}}$0.021, P:0.932	2.0043	31
(82) $[{}^{p}CH_3OC_6H_4-N=N-PO(OCH_3)_2]^{-\cdot}$	**IIId**	0.865, 0.323	^{o}0.4, ^{o}0.316, $^{m,m}2 \times 0.113$, $^{p\mathrm{CH_3O}}3 \times 0.037$, P:0.73	2.0041	31
(83) $[{}^{p}CH_3C_6H_4-N=N-PO(OCH_3)_2]^{-\cdot}$	**IIIe**	0.835, 0.360	$^{p\mathrm{CH_3}}3 \times 0.425$, ^{o}0.39, ^{o}0.305, ^{m}0.12, ^{m}0.11, P:0.89	2.0041	31
(84) $[{}^{p}CH_3COC_6H_4-N=N-PO(OCH_3)_2]^{-\cdot}$	**IIIf**		Simulation ambiguous		31
(85) $O[C_6H_4-N=N-PO(OCH_3)_2]_2^{-\cdot}$	**IIIh**	0.837, 0.356	^{o}0.45, ^{o}0.327, ^{m}0.125, ^{m}0.11, P:0.837	2.0044	31
(86) $CO[C_6H_4-N=N-PO(OCH_3)_2]_2^{-\cdot}$	**IIIi**		Mixed spectrum		31
(87) $[C_6H_5CO-N=N-COC_6H_5]^{-\cdot}$	**Xd**	2×0.588	Poorly resolved spectrum	2.0055	32
(88) $[{}^{p}ClC_6H_4CO-N=N-COC_6H_4\,{}^{p}Cl]^{-\cdot}$	**Xe**	2×0.475	Poorly resolved spectrum	2.0056	32
(89) $[{}^{p}ClC_6H_4CO-COC_6H_4\,{}^{p}Cl]^{-\cdot}$	**Xe**		$^{o,o}2 \times 0.1085$, $^{o',o'}2 \times 0.1$, $^{m,m,m,m}4 \times 0.038$	2.0056	32
(90) $[{}^{p}CH_3C_6H_4CO-N=N-COC_6H_4\,{}^{p}CH_3]^{-\cdot}$	**Xf**	2×0.487	4×0.1 (incomplete simulation)	2.0055	32

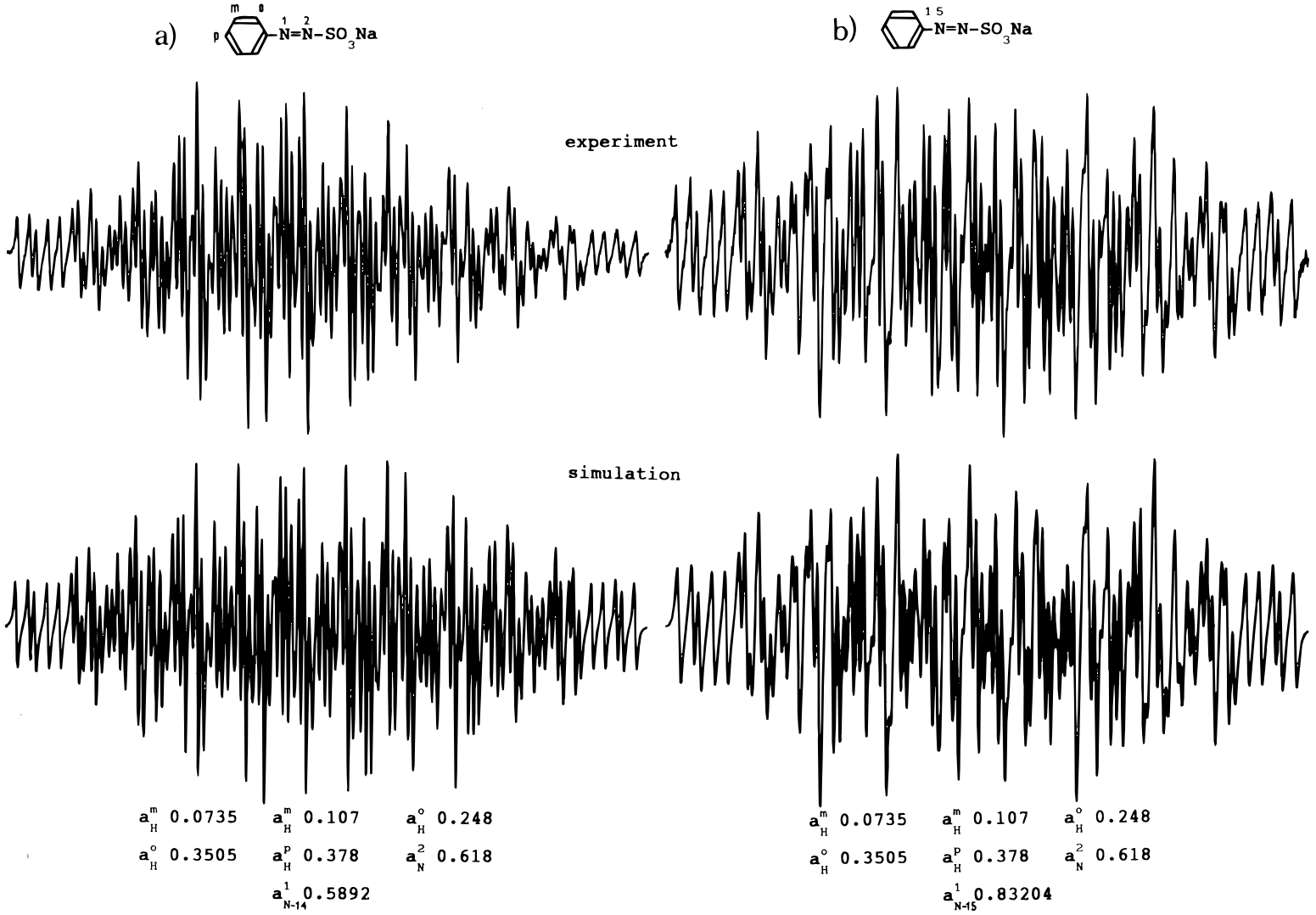

Figure 6. Experimental and simulated EPR spectra of anion radicals cathodically generated from sulfonates (a) **IVa** and (b) **IVb** in acetonitrile.

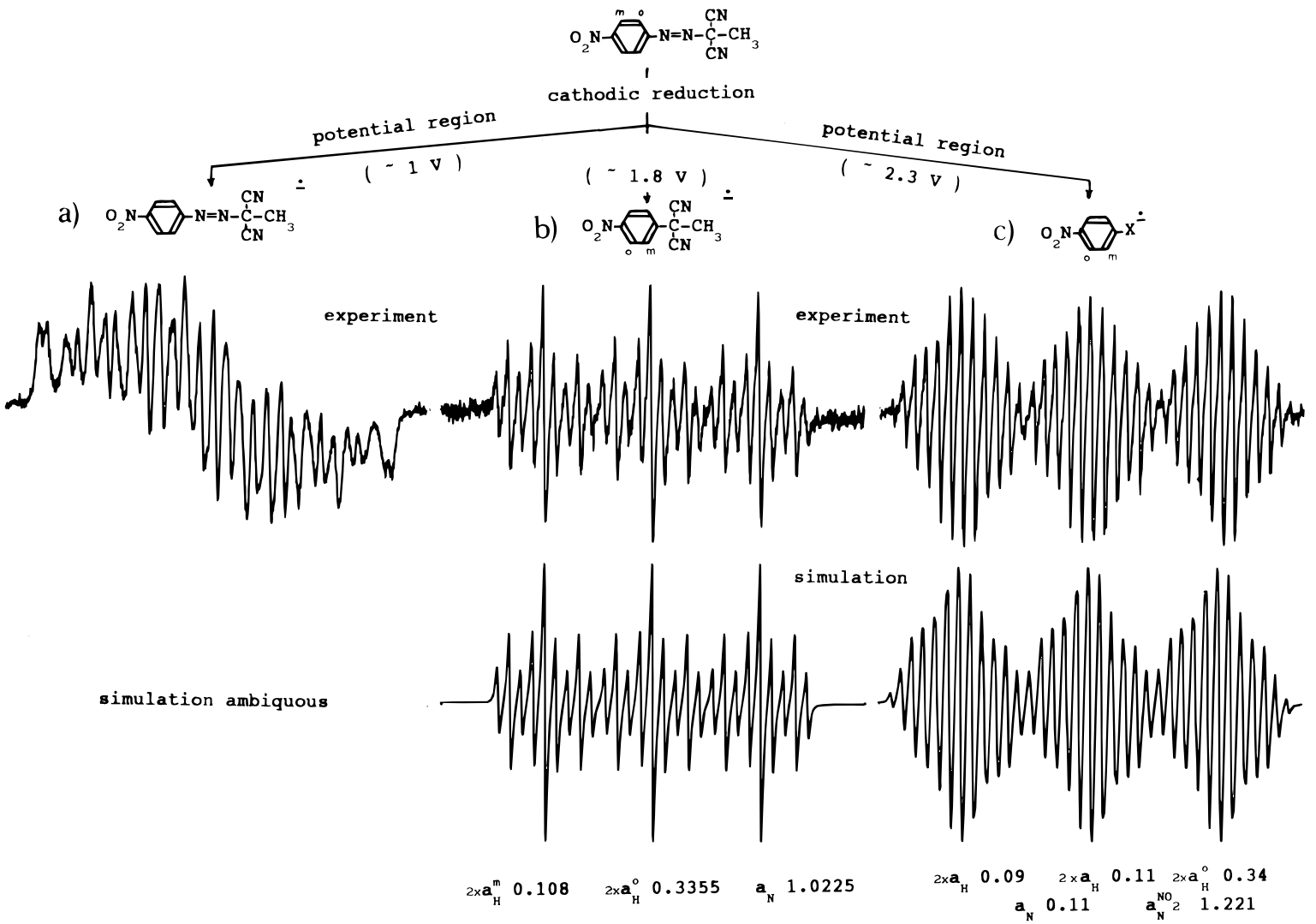

Figure 7. Experimental and simulated EPR spectra obtained at various potentials in the cathodic reduction of azo compound **IIf**.

nitrobenzene anion radicals (*p*-D and *p*-H)$C_6H_4NO_2^{-\bullet}$, the first having abstracted deuterium from CD_2Cl_2 and the second hydrogen from TBAP.

Thermal Decomposition

The investigation of thermally initiated decomposition by means of EPR spectroscopy faced some technical problems and limitations. As described in the photolytic investigations, generally the radicals formed are not stable, and the application of spin trap agents was necessary. In addition, the spin trap agents and their adducts have also only a limited thermal stability. An additional technical problem here is the time delay involved in raising the temperature of the probe to a selected value directly in the cavity of the EPR spectrometer. Therefore, only a few qualitative results will be reported here.

A significant measurable concentration of free radicals was only observed in the case of compound **IIn**, with the formation of $^{\bullet}CPh_3$ radical.

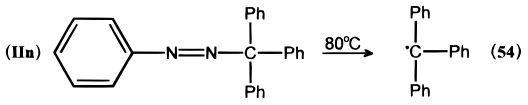

Its stability at 80 °C in toluene solution was characterized with a half-life of about 3 min, and the EPR parameters elucidated from the simulation of the experimental EPR spectrum as given in Table 2 are in agreement with those reported in the literature.[53] Generally, in thermally initiated decomposition at temperatures below 100 °C (this is the highest applicable temperature limit of the spin traps used) we usually found radical products $^1R^{\bullet}$ and $^2R^{\bullet}$ corresponding to a synchronous splitting frequently superimposed upon consecutive products of spin trap agents and their adducts. Additionally, in the case of diacylazo compounds **Xd–f** hydrazyl radicals are formed in a similar way to that described above by azosulfonates.

Free Radicals

In only a few special cases did we observe a measurable stationary concentration of the carbon- and sulfur-centered free radicals during the irradiation of the investigated azo compounds:

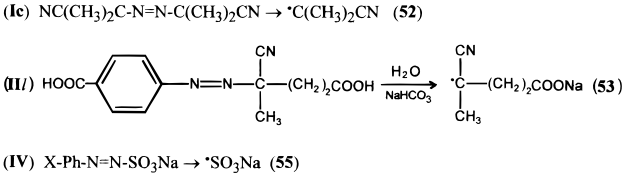

Their EPR parameters are given in Table 1. Figure 8 shows experimental and simulated EPR spectra observed in the photolysis of **Ic** in benzene [Fig. 8(a)] and **III** in aqueous solution saturated with $NaHCO_3$ [Fig. 8(b)]. The lifetime of these radicals was less than 1 s at 23 °C.

Summary of the Photochemical, Thermal and Electrochemical Stability

Table 4 qualitatively summarizes our observations on the photochemical, thermal and electrochemical stability of the investigated azo group-containing compounds **I–XII**. An extremely low thermal and photochemical

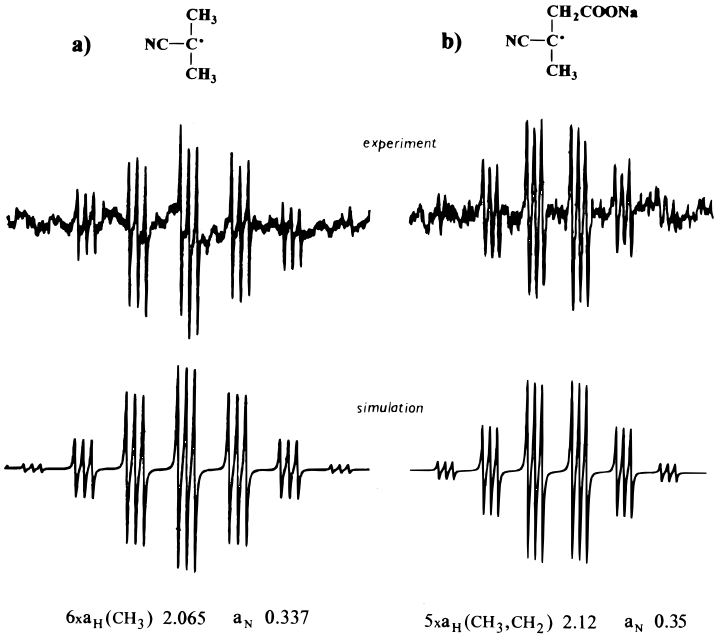

Figure 8. Experimental and simulated EPR spectra observed in the photolysis of (a) **Ic** in benzene and (b) **III** in aqueous solution saturated with $NaHCO_3$.

Table 4. Summary of the photochemical, thermal and electrochemical stability of the investigated azo group-containing compounds **I–XII** and of the radical products observed in their decomposition

Substrates	Structure	Radical products	Stability[a] UV	T	$+e^-$
I. Aliphatic azo compounds	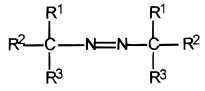	$^{\cdot}CR^1R^2R^3$ $^{\cdot}O_nCR^1R^2R^3$ (in air) $^{\cdot}OH$ (in H_2O, in air)	− −	+ −	− −
II. 1-Aryl-2-alkylazo compounds	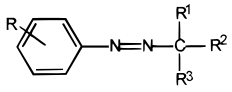	$^{\cdot}CR^1R^2R^3$, $^{\cdot}C_6H_4R$ $^{\cdot}O_nCR^1R^2R^3$ (in air) $RPh^{-\cdot}$ if R = NO_2	+ +	+ −	+ −
III. Azophosphonates	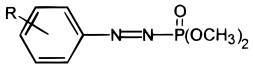	$[III]^{-\cdot}$	+ +	+ −	+ +
IV. Azosulfonates	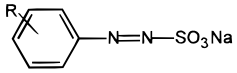	$^{\cdot}SO_3Na$ RC_6H_4—$\dot{N}$—$NXSO_3Na$ $[IV]^{-\cdot}$	+ −	+ +	+ +
V. Azosulfones	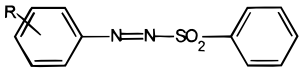	$^{\cdot}SO_2Ph$ $^{\cdot}C_6H_4R$ $[V]^{-\cdot}$	+ −	+ −	+ +
VI. Azosulfides	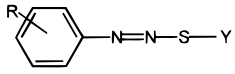	$^{\cdot}SY$ $^{\cdot}C_6H_4R$ $RPh^{-\cdot}$ if R = NO_2	+ −	+ −	+ −
VII. Triazenes	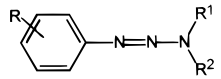	$^{\cdot}R^1$ $^{\cdot}C_6H_4R$	+ −	+ −	− −
VIII. Pentazadienes	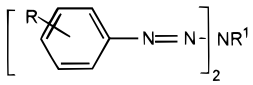	$^{\cdot}R^1$ $^{\cdot}C_6H_4R$ $^{\cdot}X(H)$	− −	+ −	− −
IX. Hexazadienes	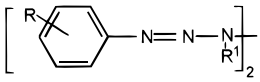	$^{\cdot}R^1$ $^{\cdot}C_6H_4R$	− −	− −	− −
X. Acyl and diacylazo compounds	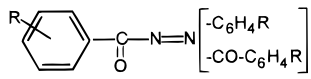	$^{\cdot}COC_6H_4R$ $^{\cdot}NX$, $[X]^{-\cdot}$ Y—$\dot{N}$—NY_2 Y = COC_6H_4R	+ −	+ −	+ +
IX. Diazonium salts	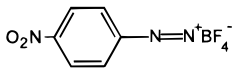	$^{\cdot}C_6H_4NO_2$ $PhNO_2^{-\cdot}$	− −	− −	− −
XII. Cyclic azo compounds	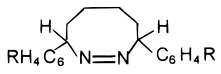	$^{\cdot}NX$	+ +	+ +	− −

[a] + +, High stability; + −, medium stability; − −, low stability.

stability was shown by aliphatic azo compounds **I** and hexazadienes **IX**. 1-Aryl-2-alkylazo compounds **II**, azosulfones **V**, azosulfides **VI** and pentazadienes **VIII** are also thermally and chemically unstable. Triazenes **VII** showed moderate photochemical decomposition and relatively high thermal stability. A limited thermally and photochemically initiated decomposition was found in the case of benzacyl-substituted azo compounds **X**, and still more stable are azophosphonates **III** and cyclic azo compounds **XII**. Azo compounds with widely conjugated groups ^1R and ^2R formed stable anion radicals in the cathodic reduction. Otherwise they decomposed by a route similar to that found for photochemically and thermally initiated decomposition, forming reactive

radicals $^1R^{\cdot}$ and $^2R^{\cdot}$ corresponding to synchronous splitting ($^1R—N_2—^2R \rightarrow {}^1R^{\cdot} + N_2 + {}^2R^{\cdot}$).

Acknowledgements

We thank the Slovak Grant Agency, Project VEGA 1/4206/97, for support of this work. The contribution of our students and co-workers cited in Refs 21–33 is gratefully acknowledged. The original figures, as specified in the legends, were published in our previous papers; we thank the publishers for the permission to use them in their original or modified form. K.E. thanks the Katholischer Akademischer Ausländer-Dienst (KAAD) for a fellowship facilitating her stay at the TU München.

REFERENCES

1. O. Nuyken and R. Weidner, *Adv. Polym. Sci.* **73/74**, 145 (1986).
2. E. G. Janzen and J. I.-P. Liu, *J. Magn. Reson.* **9**, 510 (1973).
3. E. G. Janzen, D. E. Nutter, Jr., and C. A. Evans, *J. Phys. Chem.* **79**, 1983 (1975).
4. A. J. Bard, J. C. Gilbert and R. D. Goodin, *J. Am. Chem. Soc.* **96**, 620 (1974).
5. N. Ohto, E. Niki and Y. Kamiya, *J. Chem. Soc., Perkin Trans. 2* 1770 (1977).
6. A. R. Forrester, J. Henderson and K. Reid, *Tetrahedron Lett.* **24**, 5547 (1983).
7. M. Iwamura and N. Inamoto, *Bull. Chem. Soc. Jpn.* **43**, 860 (1970).
8. E. G. Janzen and I. G. Lopp, *J. Phys. Chem.* **76**, 2056 (1972).
9. E. G. Janzen, *Creat. Detect. Excited State* **4**, 83 (1976).
10. J. Pfab, *Tetrahedron Lett.* **9**, 843 (1978).
11. P. Smith and J. S. Robertson, *Can. J. Chem.* **66**, 1153 (1988).
12. M. Kobayashi, E. Akiyama and H. Minato, *Bull. Chem. Soc. Jpn.* **47**, 1504 (1974).
13. T. Yamase, T. Ikawa, H. Kokado and E. Inoue, *Photogr. Sci. Eng.* **18**, 647 (1974).
14. R. G. Gasanov, B. V. Lopylova, L. V. Yashkina and R. Kh. Freidlina, *Izv. Akad. Nauk SSSR, Ser. Khim.* **5**, 1190 (1983).
15. G. Xu, Y. Zhao, X. Suen, Y. Liu and X. Song, *Wuli Huaxebao Xuebao* **1**, 329 (1985).
16. D. Rehorek and E. G. Janzen, *J. Prakt. Chem.* **326**, 935 (1984).
17. P. S. Engel and D. J. Bishop, *J. Am. Chem. Soc.* **97**, 6754 (1975).
18. R. Kerber, O. Nuyken and V. Pasupathy, *Makromol. Chem.* **170**, 155 (1973).
19. T. Suehiro, S. Masuda, T. Tashiro, R. Nakausa, M. Taguchi, A. Koike and A. Rieker, *Bull. Chem. Soc. Jpn.* **59**, 1877 (1986).
20. J. P. Stradins and V. T. Glezer, in *The Encyclopedia of Electrochemistry of the Elements, Organic Section*, edited by A. J. Bard and H. Lund, Vol. XIII, p. 163. Marcel Dekker, New York (1979).
21. V. Cholvad, K. Szaboová, A. Staško, O. Nuyken and B. Voit, *Magn. Reson. Chem.* **29**, 402 (1991).
22. A. Staško, K. Szaboová, V. Cholvad, O. Nuyken and J. Dauth, *J. Photochem. Photobiol. A* **69**, 295 (1993).
23. A. Staško, O. Nuyken, B. Voit and S. Biskupič, *Tetrahedron Lett.* **31**, 5737 (1990).
24. A. Staško, V. Adamčík, T. Lippert, A. Wokaun, J. Dauth and O. Nuyken, *Makromol. Chem.* **194**, 3385 (1993).
25. K. Erentová, A. Staško, C. Scherer, B. Voit and O. Nuyken, *Chem. Pap.* **50**, 60 (1996).
26. J. Stebani, PhD Thesis, Universität Bayreuth (1993).
27. R. Kublickas, unpublished results.
28. Th. Lippert, PhD Thesis, Universität Bayreuth (1992).
29. P. Rapta, A. Staško, D. Bustin, O. Nuyken and B. Voit, *J. Chem. Soc., Perkin Trans. 2* 2049 (1992).
30. K. Erentová, V. Adamčík, A. Staško, O. Nuyken and A. Lang, *Collect. Czech. Chem. Commun.* **62**, 855 (1997).
31. K. Erentová, L. Omelka, A. Staško, C. Scherer and O. Nuyken, in preparation.
32. K. Erentová, PhD Thesis, Universität München (1997).
33. R. Bayer, PhD Thesis, Universität Bayreuth (1994).
34. E. G. Janzen and B. J. Blackburn, *J. Am. Chem. Soc.* **90**, 5909 (1968).
35. G. R. Chalfont, M. J. Perkins and A. Horsfield, *J. Am. Chem. Soc.* **90**, 7141 (1968).
36. C. Lagercrantz and S. Forschult, *Nature* (*London*) **216**, 1247 (1968).
37. A. Baindl, A. Lang and O. Nuyken, *Makromol. Chem. Phys.* **197**, 4155 (1996).
38. O. Nuyken, C. Scherer and B. Voit, *Makromol. Chem. Phys.* **197**, 1101 (1996).
39. U. Krynitz, F. Gerson, N. Wiberg and M. Weith, *Angew. Chem., Int. Ed. Engl.* **8**, 755 (1969).
40. R. Sustmann and R. Sauer, *J. Chem. Soc., Chem. Commun.* 1248 (1985).
41. Ch. J. Rhodes, *J. Chem. Soc., Faraday. Trans. 1* 3215 (1988).
42. F. Williams, Q.-X. Guo, P. A. Petillo and S. F. Nelsen, *J. Am. Chem. Soc.* **110**, 7887 (1988).
43. F. Gerson and X.-Z. Qin, *Helv. Chim. Acta* **71**, 1498 (1988).
44. M. E. Mendicino and S. C. Blackstock, *J. Am. Chem. Soc.* **113**, 713 (1991).
45. G. Gescheidt, A. Lamprecht, C. Ruchardt and M. Schmittel, *Helv. Chim. Acta* **74**, 2094 (1991).
46. C. H. Ess, F. Gerson and W. Adam, *Helv. Chim. Acta* **74**, 2078 (1991).
47. C. H. Ess, F. Gerson and W. Adam, *Helv. Chem. Acta* **75**, 335 (1992).
48. R. J. Bushby and K. M. Ng, *J. Chem. Soc., Perkin Trans. 2* 1053, 1525 (1996).
49. E. T. Strom, G. A. Russell and R. Konaka, *J. Chem. Phys.* **42**, 2033 (1965).
50. N. M. Atherton, F. Gerson and J. N. Ockwell, *J. Chem. Soc. A* 109 (1966).
51. A. G. Evans, J. C. Evans, P. J. Emes, C. L. James and P. J. Pomery, *J. Chem. Soc. B* 1484 (1971).
52. F. A. Neugebauer and H. Weger, *Chem. Ber.* **108**, 2703 (1975).
53. (a) *Landolt-Bornstein, New Series II/9b*, p. 719. Springer, Berlin (1977); (b) *Landolt-Bornstein, New Series II/17b*, p. 253. Springer, Berlin (1987).

